Spatial angle dependent lasing from a dye-doped two-dimensional hexagonal photonic crystal made of holographic polymer-dispersed liquid crystals

D. Luo,[1] H. T. Dai,[2] H. V. Demir,[1,3,4] X. W. Sun,[1,2*] H. Z. Yang,[5] and W. Ji[5]

[1]School of Electrical and Electronic Engineering, Nanyang Technological University, Nanyang Avenue, Singapore 639798, Singapore
[2]Department of Applied Physics, College of Science, and Tianjin Key Laboratory of Low-Dimensional Functional Material Physics and Fabrication Technology, Tianjin University, Tianjin 300072, China
[3]School of Physical and Mathematical Sciences, Nanyang Technological University, Nanyang Avenue, Singapore 639798, Singapore
[4]Department of Electrical and Electronics Engineering and Department of Physics, UNAM – Institute of Materials Science and Nanotechnology, Bilkent University, Bilkent, Ankara, 06800 Turkey
[5]Department of Physics, National University of Singapore, 2 Science Drive 3, Singapore 117542, Singapore
[*]exwsun@ntu.edu.sg

Abstract: The observation of spatial angle dependent lasing from a dye-doped two-dimensional photonic crystal (2D PC) holographic polymer dispersed liquid crystals made of hexagonal lattice structure is reported. With the increasing output angle of the laser beam in the plane perpendicular to the 2D PC, the lasing wavelength is red-shifted. By analyzing the lasing oscillation trace, we found that the effective lattice constant changes with the output angle, causing the spatial angle dependent lasing.

©2012 Optical Society of America

OCIS codes: (140.3460) Lasers; (160.5298) Photonic crystals; (160.3710) Liquid crystals.

References and links

1. E. Yablonovitch, "Inhibited spontaneous emission in solid-state physics and electronics," Phys. Rev. Lett. **58**(20), 2059–2062 (1987).
2. J. D. Joannopoulos, R. D. Meade, and J. N. Winn, *Photonic crystals: molding the flow of light* (Princeton University Press, 1995).
3. T. J. Bunning, L. V. Natarajan, V. P. Tondiglia, and R. L. Sutherland, "Holographic polymer-dispersed liquid crystals (H-PDLCs)," Annu. Rev. Mater. Sci. **30**(1), 83–115 (2000).
4. Y. J. Liu and X. W. Sun, "Electrically tunable two-dimensional holographic photonic crystal fabricated by a single diffractive element," Appl. Phys. Lett. **89**(17), 171101 (2006).
5. R. L. Sutherland, V. P. Tondiglia, L. V. Natarajan, S. Chandra, D. Tomlin, and T. J. Bunning, "Switchable orthorhombic F photonic crystals formed by holographic polymerization-induced phase separation of liquid crystal," Opt. Express **10**(20), 1074–1082 (2002).
6. K. Sakoda, "Enhanced light amplification due to group-velocity anomaly peculiar to two- and three-dimensional photonic crystals," Opt. Express **4**(5), 167–176 (1999).
7. G. S. He, T.-C. Lin, V. K. S. Hsiao, A. N. Cartwright, P. N. Prasad, L. V. Natarajan, V. P. Tondiglia, R. Jakubiak, R. A. Vaia, and T. J. Bunning, "Tunable two-photon pumped lasing using a holographic polymer-dispersed liquid-crystal grating as a distributed feedback element," Appl. Phys. Lett. **83**(14), 2733–2735 (2003).
8. R. Jakubiak, L. V. Natarajan, V. Tondiglia, G. S. He, P. N. Prasad, T. J. Bunning, and R. A. Vaia, "Electrically switchable lasing from pyrromethene 597 embedded holographic-polymer dispersed liquid crystals," Appl. Phys. Lett. **85**(25), 6095–6097 (2004).
9. R. Jakubiak, V. P. Tondiglia, L. V. Natarajan, R. L. Sutherland, P. Lloyd, T. J. Bunning, and R. A. Vaia, "Dynamic lasing from all-organic two-dimensional photonic crystals," Adv. Mater. (Deerfield Beach Fla.) **17**(23), 2807–2811 (2005).
10. D. Luo, X. W. Sun, H. T. Dai, Y. J. Liu, H. Z. Yang, and W. Ji, "Two-directional lasing from a dye-doped two-dimensional hexagonal photonic crystal made of holographic polymer-dispersed liquid crystals," Appl. Phys. Lett. **95**(15), 151115 (2009).

11. D. Luo, X. W. Sun, H. T. Dai, H. V. Demir, H. Z. Yang, and W. Ji, "Electrically tunable lasing from a dye-doped two-dimensional hexagonal photonic crystal made of holographic polymer-dispersed liquid crystals," Appl. Phys. Lett. **97**(8), 081101 (2010).
12. D. Luo, X. W. Sun, H. T. Dai, H. V. Demir, H. Z. Yang, and W. Ji, "Temperature effect on the lasing from a dye-doped two-dimensional hexagonal photonic crystal made of holographic polymer-dispersed liquid crystals," J. Appl. Phys. **108**(1), 013106 (2010).
13. M. Notomi, "Theory of light propagation in strongly modulated photonic crystals: refractionlike behavior in the vicinity of the photonic band gap," Phys. Rev. B **62**(16), 10696–10705 (2000).

1. Introduction

Photonic crystals (PCs) are periodic optical structures designed to control the flow of photon [1, 2]. Two-dimensional (2D) and three-dimensional (3D) PCs based on holographic polymer-dispersed liquid crystals (H-PDLCs) [3] have recently received great attention [4, 5]. Due to the low refractive index contrast, H-PDLC PCs generally cannot form complete photonic bandgaps as the PCs fabricated using semiconductor materials. However, the local field enhancement is still possible inside the H-PDLC PCs through the group-velocity anomaly [6], and lasing action can be generated in a relatively wider range on photonic band, rather than photonic band edge in the case of photonic crystal with high refractive index contrast. The group-velocity anomaly, where the group velocity becomes small over a wide range of wave vectors, is absent in one-dimensional (1D) case and peculiar to 2D and 3D PCs even with a rather small index contrast.

Laser emissions from dye-doped H-PDLC have been reported in 1D (gratings) [7, 8] and 2D PCs [9, 10]. For dye-doped photonic crystal, the photonic crystal structure formed by H-PDLC acts as an optical cavity, while the doped dye molecules act as the laser gain medium. The electrically tunable and temperature dependent characteristics of lasing from dye-doped 2D H-PDLC PCs are also investigated [11, 12]. However, to our knowledge, the angle dependent lasing from a 2D H-PDLC PC has never been reported. In this paper, we shall investigate the angular dependence of lasing from dye-doped 2D H-PDLC PCs with a hexagonal lattice structure. We show that the lasing spectrum is dependent on the output angle of the laser beam. The root cause of the lasing spectrum shift is the different effective lattice constant experienced by different lasing oscillations.

2. Experiment

In our experiment, the LC/prepolymer mixture syrup, which was used to fabricate the dye-doped 2D PC with hexagonal lattice structure, consisted of 53.10 wt% monomer, trimethylolpropanetriacrylate (TMPTA), 13.14 wt% cross-linking monomer, *N*-vinylpyrrollidone (NVP), 0.72 wt% photoinitiator, Rose Bengal (RB), 1.09 wt% coinitiator, *N*-phenylglycine (NPG), 10.95 wt% surfactant, octanoic acid (OA), and 1.82 wt% lasing dye, 4-dicyanomethylene-2-methyl-6-p-dimethylaminostyryl-4H-pyran (DCM), all from Sigma-Aldrich, and 19.18 wt% liquid crystal, E7 (n_o = 1.521 and n_e = 1.7462), from Merck [10]. The mixture was filled into a cell, formed by indium tin oxide (ITO) glass, by capillary action. The 2D PC was holographically fabricated through the three-beam interference generated by a specially designed prism.

Fig. 1(a) shows the schematic of the prism used. The bottom plane (equilateral triangle) of the prism has a side length of BC = BD = CD = 6 cm, and a side-bottom plane angle of Φ = 60°. A collimated Ar + laser beam (514.5 nm) impinged normally onto the prism, and three beams, k_1, k_2, and k_3 (Fig. 1 (b)) emerged through the refraction from three tilted side surfaces of the prism, where k represents wave vector, θ represents the angle between the wave vector and *z* axis, and φ represents the angle between the projection of wave vector on *x-y* plane and *x* axis. Here we have $\theta_1 = \theta_2 = \theta_3 = \theta$ = 25.3° and φ_1 = 0, φ_2 = 120°, φ_3 = 240° [10]. The cell filled with LC/prepolymer mixture was attached onto the bottom surface through an index-matching liquid for recording the interference pattern, as shown in Fig. 1(c).
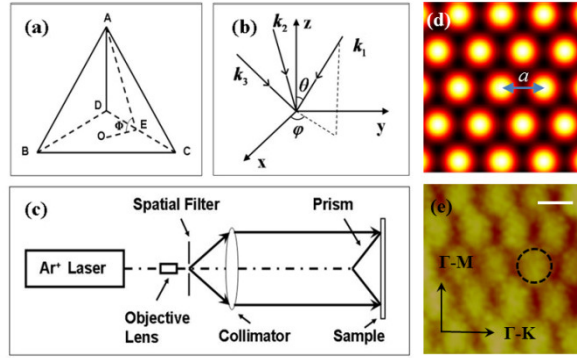
Fig. 1. (a) The specially designed prism, (b) three-beam interference configuration, and (c) schematic of the optical setup [10]. (d) Simulated intensity distribution of the three-beam interference pattern. (e) AFM image showing the surface morphology of the 2D hexagonal H-PDLC PCs. Scalar bar: 500 nm.

Assuming the three beams have the same phase, the intensity distribution of the interference pattern can be defined as [10]:

$$\mathrm{I}(r) = \Re\left(\sum_{i,j=1}^{3} \mathrm{E}_i \cdot \mathrm{E}_j \exp[i(\mathrm{k}_i - \mathrm{k}_j)\cdot \mathrm{r}] \right), \qquad (1)$$

where E is the amplitude, $r = (x, y, z)$ is a position vector, and $\Re[\ldots]$ denotes the real part of the argument. For three beams with equal intensity, $E_1 = E_2 = E_3$, the simulated interference pattern in x-y plane is shown in Fig. 1(d), where the red- and black-color areas represent high and low intensities, corresponding to polymer-rich and LC-rich regions respectively when it was recorded in the PDLCs [10]. The lattice constant is given by $\mathrm{a}_0 = 2\lambda / (3n\sin\theta)$, where λ = 514.5 nm, n = 1.537 (calculated according to the ratio of polymer and LC), and $\theta = 25.3°$. The theoretical lattice constant is calculated to be 522 nm [10]. Fig. 1(e) shows the sample's surface morphology checked by an atomic force microscope (AFM). The estimated lattice constant was ~500 nm and the polymer columns (marked by the dash circle) have a radius of ~145 nm. The experimental lattice constant (500 nm) was in good agreement with the prediction (522 nm), considering a general 5% volume shrinkage for acrylate monomers during Photopolymerization [10].

Fig. 2 shows the optical setup of the lasing experiment and the resulting output spectrum. Laser emissions along ΓM (y axis) directions in the sample took place when it was optically excited by a Q-switched frequency-doubled Nd:yttrium-aluminum-garnet (Nd:YAG) pulsed laser operating at 532 nm with a pulse duration of 7 ns at a repetition rate of 10 Hz. A linearly polarized pumping laser, focused by a cylindrical lens, was incident on the surface of the sample along the z direction. The pumping power was fixed at 250 μJ/pulse. A fiber coupled spectrometer with a resolution of 0.6 nm was used to collect the lasing output.

The lasing spectrum was first measured near the sample at point N (about 1 mm away from the sample, see Fig. 2), where multiple peaks were found within a broad range from 606.0 to 627.6 nm. Both TE and TM modes existed in the lasing with similar intensities. Although the multi-peak lasing generation within H-PDLC is expected according to the previous reports of theoretical simulation [6] and experimental works [10–12], lasing in such a wide range has never previously been observed (previously lasing peaks were generally within a spectral range of less than 10 nm, measured at distance of about 1~2 cm away from the sample). Further moving the spectrometer far away from the sample to a distance of about 6 cm, the spatial pattern of the output laser beam is found to be separated into two spots, which are symmetric with respect to the x axis, and similar to a traditional rectangle

transverse mode pattern TEM_{10} generated from a laser cavity with rectangle symmetry. One magnified laser spot image is shown in Fig. 2 (upper left). Here the lasing spectra were measured at several different points from A to F. The measurements at two other positions C_1 and C_2 were also carried for comparison purpose. The middle point of these two laser spots is labeled by O.
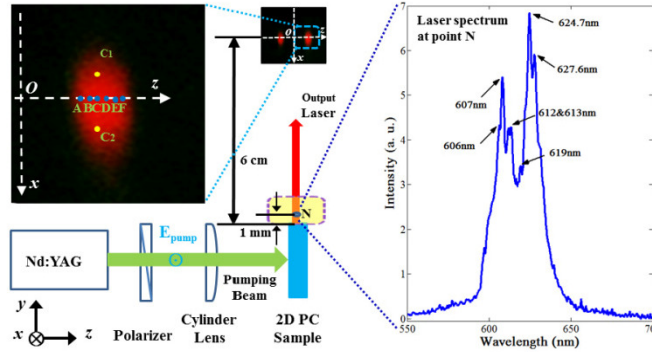

Fig. 2. Optical setup of the lasing experiment. The laser spectrum on the right side is measured near the sample at point N (1 mm away from the sample). The laser image obtained on a screen at the far distance of 6 cm away from the sample is shown, along with a magnified image of one of the laser spots zoomed in the upper left. The measured positions were marked from A to F along the horizontal z axis, as well as the additional points $C1$ and $C2$ for comparison purpose. The point O is marked on the midline.

3. Results and discussions

Figs. 3(a)-(f) show the measured lasing spectra from position A to F, respectively. The lasing spectrum obtained at point N is also presented for comparison purpose. At the position A, the lasing peaked at the shortest wavelength of 606.0 nm. The lasing peak moved toward longer wavelengths while measure position shifted from A to F. Lasing peaks of 607.0 nm, 612.0 nm, 618.0/619.0/620.8 nm, 619.0/624.7 nm, and 619.0/624.7/625.8/627.6 nm were observed from position B to F, respectively. The relationship of peak intensity verse pumping power is shown in each inset figure. The thresholds of 180 μJ/pulse were achieved for all points except point D, where the threshold is 210 μJ/pulse. It is also worth mentioning that no shift in the lasing peaks was observed, while measure position vertically shifted from C to C_1 and C_2, indicating the lasing spectrum shifting only happened along the z direction.

From Fig. 3, we can see that, beside the lasing peak wavelength, the measured intensity of each lasing spectrum at the far distance is also close to the intensity measured at the near distance (point N), implying that the spectrum obtained at the near distance is a simple summation of the lasing spectra obtained at the far distance. The laser beam trace inside the H-PDLC sample can explain this experimental phenomenon. The different intensity for lasing spectrum at different angle is primarily due to the photonic crystal slab modes.

Fig. 4(a) shows the pumping, output and coordination system of the PC sample. The cross section of the y-z plane is sketched in Fig. 4(b), where two possible laser light traces are represented by the red solid lines, labeled as a and f. As shown in Fig. 4(b), inner trace angle γ is defined as the angle between the laser light trace and the y axis inside H-PDLC, while output angle β is the refraction angle of the laser beam trace in air. Lines a and f represent the light traces with the smallest and largest output angles, corresponding to the position of A and F in Fig. 4 (a), respectively. The PC lattice constant is fixed to be a_0, which corresponds to the trace with zero inner trace angle (dash line in Fig. 4(b), parallel to the y axis). For other traces, the effective lattice constant is defined as $a_{eff\_i} = a_0/\cos\gamma_i$ ($i = a, b, …f$), which varies with the inner trace angle γ_i.

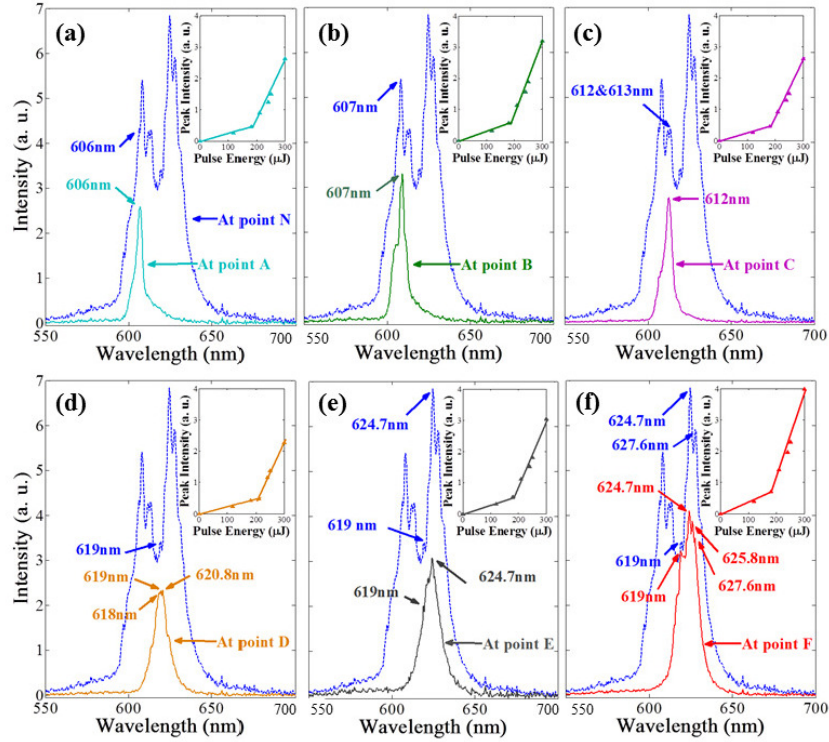Fig. 3. Lasing spectrum measured at the far positions from *A* to *F* (all at a surface-normal distance of 6 cm), with the pumping power of 250 μJ/pulse: (a)-(f), corresponding to the spectrum measured at the position of *A* to *F*, respectively. All of these figures also show the spectrum recorded at point *N* (in dashed lines) on the background for comparison purpose. The inset figure shows the relationship of peak intensity verse pumping power.

The far point is 6 cm away from the sample, meaning PO = 6 cm, where P is the interface point of H-PDLC sample and air on the horizontal line. The distances between points *A* and *F* to O are AO = 1.71 cm and FO = 3 cm, respectively. β_a and β_f, the output angles of the light traces *a* and *f*, are calculated to be 15.91°, and 26.57°, respectively. According to the Snell's law, we have

$$n_{air} \sin \beta = n_{H-PDLC} \sin \gamma \qquad (2)$$

where n_{air} = 1, and $n_{H\text{-}PDLC}$ = 1.537. γ_a and γ_f are calculated to be 10.27°, and 16.92°, respectively. According to the relationship $a_{eff\_i} = a_0/\cos\gamma_i$, we obtained a_{eff_a} = 1.016a_0 and a_{eff_f} = 1.045a_0. Similarly, we had a_{eff_b} = 1.021a_0, a_{eff_c} = 1.027a_0, a_{eff_d} = 1.033a_0, and a_{eff_e} = 1.039a_0.

Therefore, different light traces have different inner trace angles γ, leading to different effective lattice constants, and consequently yield to different lasing spectra measured at different positions.

To understand the relationship of the lasing peak wavelength and effective lattice constant, we studied the photonic band structure of our sample. Fig. 4(c) shows the calculated photonic band structures for TE/TM polarization in the 2D hexagonal HPDLC PC using the plane wave expansion method [13], where the used parameters include polymer column radius r = 0.29a_{eff}, n_p = 1.522, n_{LC} = 1.597. In Fig. 4(c), the vertical axis a_{eff}/λ is the ratio of effective lattice constant and wavelength. For positions *A* and *F*, the calculated a_{eff}/λ are a_{eff_a}/λ = 1.016 × 500/606 = 0.838 and a_{eff_f}/λ = 1.045 × 500/624.7 = 0.836, respectively, where the lasing

peak central wavelength are selected. For other positions from *B* to *E*, we obtained a_{eff_b-e}/λ = 0.841, 0.839, 0.834, and 0.832, respectively.
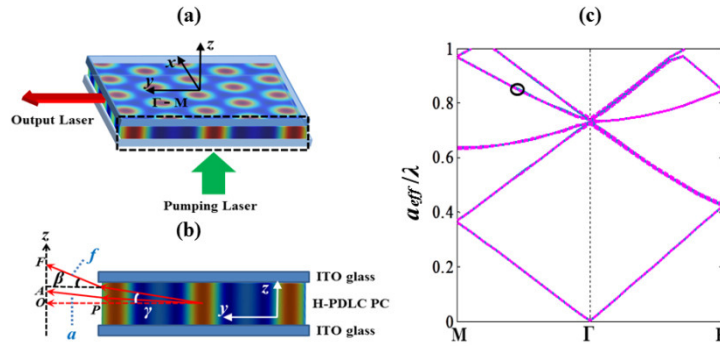

Fig. 4. (a) Structure of the H-PDLC PC sample shown with the directions of pumping and output laser. (b) Cross-section of the *y-z* plane of the H-PDLC PC sample (dash rectangle in (a)). *γ* and *β* represents the incident angle in the sample and the output angle outside the sample, respectively. Different laser beams are represented by the solid red lines labeled *a* and *f*. (c) Photonic band structure of the 2D H-PDLC PC with a hexagonal lattice. Both TE and TM polarizations are represented. The lasing generation region is marked by a circle.

From the calculated results, we can see that the normalized frequency fluctuates around 0.837 with a maximum difference of less than 0.6% when the measurement position is displaced from position *A* to *F*, showing a high degree of stability. Considering the inevitable measurement errors in data collection, we can conclude that for all different lasing traces, the a_{eff}/λ is kept almost unchanged, meaning that all the lasing emissions were stimulated under similar conditions, such as group velocity dispersion and local field enhancement. This explanation for spatial angle dependent lasing is reasonable and confirmed by our experiments. Therefore, the red shift in the lasing spectrum, while measured from positions *A* to *F*, should be attributed to the increased effective lattice constant, which in turn stems from an increased incident angle of the laser oscillation trace within the H-PDLC PC sample.

4. Conclusion

In conclusion, we studied and understood the spatial angle dependence of lasing from dye-doped 2D H-PDLC PCs with a hexagonal lattice structure. A red-shifting lasing spectrum is observed with the increasing output angle of the laser beam. The different effective lattice constant of the PC structure experienced by different lasing oscillation traces is found to be the underlying reason of this spatial angle dependent lasing.

Acknowledgments